LANGMUIR

pubs.acs.org/Langmuir Article

Mechanical Stability of DNA Corona Phase on Gold Nanospheres

Pravin Pokhrel, Kehao Ren, Hao Shen, and Hanbin Mao*



Cite This: Langmuir 2022, 38, 13569-13576



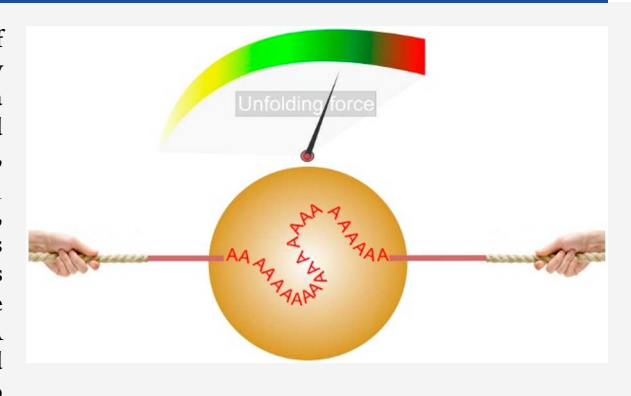
ACCESS I

III Metrics & More

Article Recommendations

Supporting Information

ABSTRACT: Noncovalent adsorption of biopolymers on the surface of gold nanoparticles (AuNPs) forms a corona phase that drastically diversify AuNP functions. However, mechanical stabilities of such corona phase are still obscure, hindering the application of biopolymer-coated AuNPs. Here, using optical tweezers, we have observed, for the first time, that DNA corona phase adsorbed on a 5 nm AuNP via two (dA)₂₁ strands in proximity can withstand an average desorption force of 40 pN, which is higher than the stall force of DNA/RNA polymerases. This suggests a new role for AuNPs to modulate replications or transcriptions after binding to prevalent poly(dA) segments in eukaryotic genomes. We have also revealed that with increasing AuNP size (1.8–10 nm), DNA corona becomes harder to remove, likely due to the larger surfaces and flatter facets on bigger AuNPs. These findings provide guidance to



design AuNP corona that can withstand harsh environments for biological and materials applications.

■ INTRODUCTION

With tunable physical and chemical properties, gold nanoparticles (AuNPs) have demonstrated versatile applications across many fields.^{1–3} In particular, because of their versatile biofunctionalities and easy derivatization with bioactive molecules, AuNPs have been widely employed in the biomedical applications.^{1,4} Functionalization of AuNPs plays an essential role to modulate activities of AuNPs. A diverse set of molecules such as proteins,^{5,6} nucleic acids (DNA or RNA),^{7–9} and organic molecules^{10,11} can be conjugated to the AuNP surface, drastically expanding the applications of AuNPs.

Among different functionalization strategies, anchoring DNA molecules onto AuNPs represents a particularly attractive approach due to the biocompatibility, functional diversity, and bottom-up programmability in DNA. 7,9,12 However, since both DNA and AuNPs are negatively charged, challenge exists to overcome their charge repulsion while maintaining the stability of AuNP colloids. 7,12 Salt-aging and pH-based DNA loading are among the first techniques to functionalize thiolated DNA on gold nanospheres. 7,13-15 These processes are tedious to perform and require chemical modification of DNA with a sulfhydryl group. Recently, it has been found that natural polydeoxyadenosine (poly(dA)) can adsorb to AuNP surfaces to form a DNA corona phase via noncovalent Au–N interactions 16-20 using either salt-aging 17 or low-pH-assisted²¹ procedures. This strategy has been further streamlined using a simple freeze-and-thaw procedure to displace original AuNP coating ligands with poly(dA) within 15 min. 22

When AuNPs are used in biological environment, it becomes important to maintain a stable corona surface for

bioavailability while preserving desired activities of AuNPs. Research has found that thermodynamic stability of coated ligands on AuNPs depends on the nanoparticle size, salt concentration, and buffer pH. ^{23–27} Several studies in the past have revealed mechanical stabilities of covalent Au–S interactions. ^{28,29} Dependent on the sulfhydryl group in various molecules, ^{30,31} rupture forces up to 1.5 nN have been detected, which may come from the rupture events of Au–Au atoms, instead of Au–S bonds. ³⁰

However, the mechanical stability of noncovalently adsorbed corona phase, such as the poly(dA) coating on AuNPs, is yet to be revealed. Because of rather convenient procedures, these noncovalent adsorptions recently have been exploited to prepare multidomain AuNP containing nanodevices with hierarchical structures and functionalities. Given that many applications of AuNPs occur in hydrogels and polymers that may experience high mechanical stresses such as swelling and shrinking, as well as centrifugation and shear flows, it becomes urgent to reveal mechanical properties of the corona phase on the AuNPs. In this work, we have studied the mechanical stability of noncovalent Au–N based corona adsorption for the first time using optical tweezers. Given the high sensitivity of optical tweezers in the mechanical force measurement, and its superiority over other force spectroscopy

Received: August 22, 2022 Revised: October 14, 2022 Published: October 28, 2022





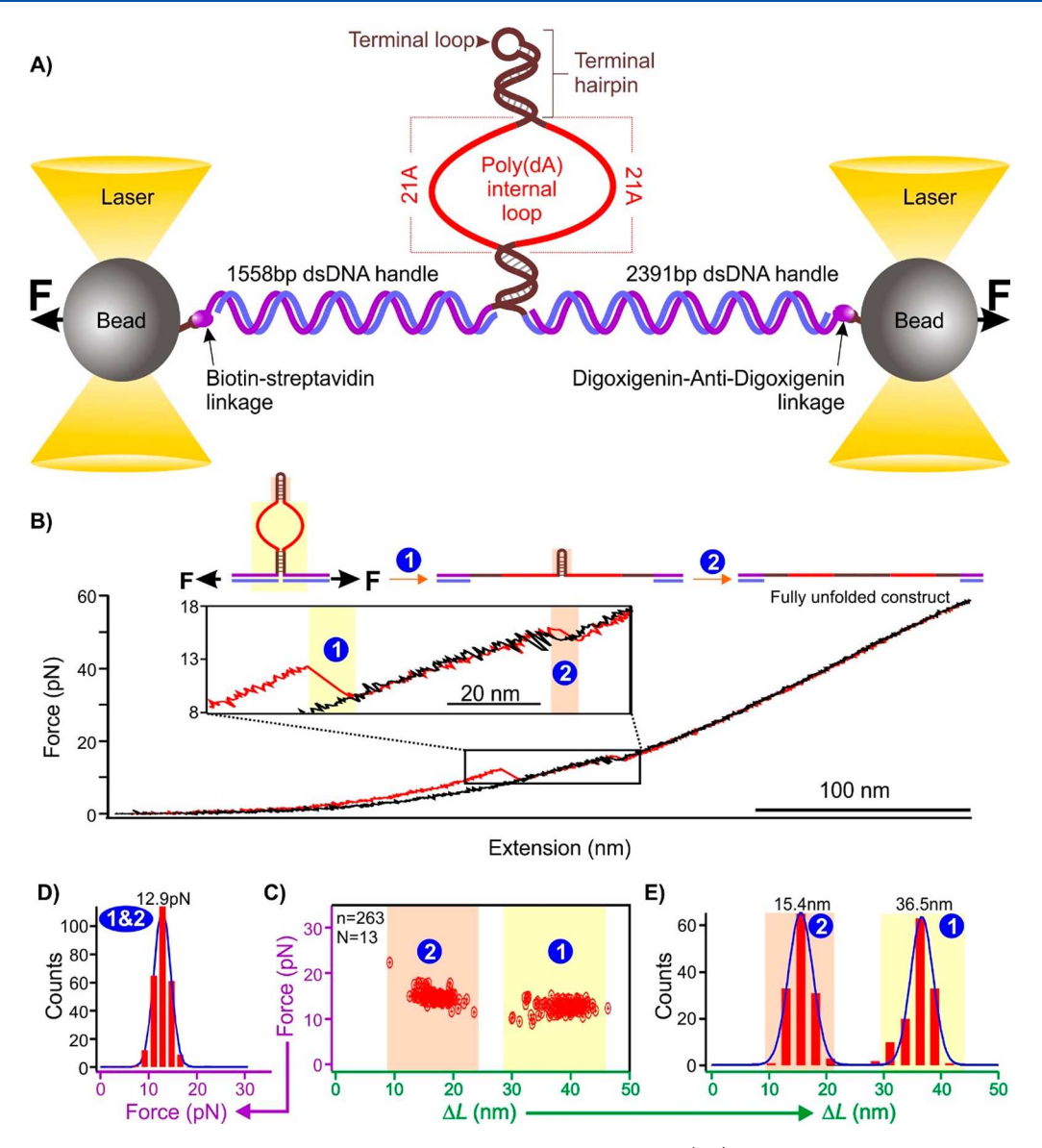


Figure 1. (A) Schematic of the single-molecule platform to investigate the binding of poly(dA) to gold nanospheres. See Table S1 in the SI for DNA sequences. (B) A typical force extension curve when a DNA construct is stretched (red) and relaxed (black) in the optical tweezers instrument. (C) Scatter plot of force vs change-in-contour-length (ΔL). (D) Unfolding force and (E) change-in-contour-length (ΔL) histograms of the unfolding features shown in panel (C). Solid curves are Gaussian fittings. N represents the number of molecules from which the FX curves were collected, and n represents the total number of unfolding features measured.

methods to minimize surface effect,³⁴ we used this method to study the mechanical stability of DNA corona phase on AuNPs. Based on the widely used poly(dA)-AuNP conjugates, we have found that two $(dA)_{21}$ strands in close proximity show much improved adsorption to AuNPs than one $(dA)_{21}$ strand or strands with shorter poly(dA) segments.

We have observed that a desorption force of >20 pN (average 37–43 pN) is needed to break the noncovalent interaction between the DNA and AuNPs. This mechanical stability is lower than that of covalent Au–S bonds, which is in the range of several hundreds to >1000 pN. ^{30,31} However, it is higher than that to maintain DNA secondary structures such as duplexes and tetraplexes (<~20 pN^{35,36}) or to stall motor proteins such as DNA or RNA polymerases. ^{37–39} As DNA duplexes and tetraplexes routinely exist inside cells, ⁴⁰ this suggests that AuNP coated with poly(dA) corona phase is strong enough to withstand the cellular environment from a

mechanical perspective. Since poly(dA) is ubiquitous in genomes, $^{41-43}$ a new function of AuNP may exist to modulate replication or transcription processes via binding to the poly(dA) segments.

■ RESULTS AND DISCUSSION

Single-Molecule Setup To Study the Poly(dA) Corona on Gold Nanospheres. To investigate the noncovalent binding of poly(dA) DNA to AuNP, we designed a DNA construct consisting of a hairpin with two (dA)₂₁ internal loops in the stem (shown in red in Figure 1A). In the microfluidic chamber in optical tweezers instrument (see section S9 in the Supporting Information (SI)), the hairpin was tethered between two optically trapped beads using 1558 bp and 2391 bp dsDNA handles. The tethering was achieved by biotin/streptavidin and digoxigenin/antidigoxigenin affinity interactions (detailed synthesis of the construct can be found

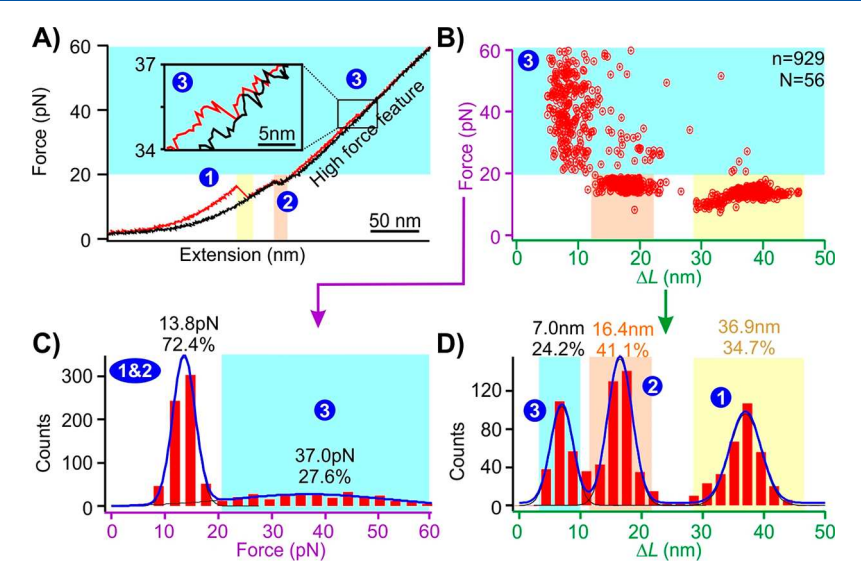


Figure 2. (A) A typical force extension curve when the DNA construct (shown in Figure 1) is stretched (red) and relaxed (black) in the presence of a 5 nm AuNP. A new unfolding feature (marked as "3") is observed in the presence of nanogold. (B) Plot of the unfolding force vs ΔL of the unfolding events. (C and D) Unfolding force and ΔL histograms of the features in the presence of the 5 nm AuNP, respectively. Solid curves are Gaussian fittings. N represents the number of molecules from which the FX curves were collected, and n represents the total number of unfolding features measured.

in Figures S1 and S2 in the SI). Tension in the DNA construct was developed when the two optically trapped beads were moved apart by steering one of the trapping lasers. When the tension was sufficiently high, the hairpin was unfolded, generating distinct unfolding features in the force-extension (FX) curve as shown in Figure 1B. The internal loops were ripped apart before the unfolding of the terminal hairpin, since the former experienced the tension before the latter did, because of their relative locations with respect to the direction of the applied force. Upon relaxing the stretched DNA construct to ~12.9 pN, the unfolded terminal hairpin refolded faster than the rest of the structure, because of its small size and close proximity of the two complementary hairpin stems. The region below the terminal hairpin did not show immediate refolding during relaxation due to a long noncomplementary region made of (dA)₂₁ in each internal loop. However, given sufficient time (\sim 15 s) at zero force, the complementary region below the poly(dA) internal loop refolded completely and the rupture feature was observed again in the next FX curve. The forces to unfold the internal loops and the terminal hairpin were centered at 12.9 pN (Figures 1 C and 1D), which is close to the unzipping force of duplex DNA.^{35,44} In the change-incontour-length (ΔL) histogram (Figures 1 C and 1E), two distinct populations represent the unfoldings of the terminal hairpin ($\Delta L = 15.4$ nm) and the internal loops ($\Delta L = 36.5$ nm), respectively. While the unfolding to release the internal loops shows the ΔL (36.5 nm) close to that expected (39.6 nm, see Figure S7 in the SI), the terminal hairpin gives a smaller ΔL value (15.4 nm) compared to that expected (22.3 nm), which may be due to the breathing of the duplex DNA at the end of hairpin stems. 35,45

Adsorption of DNA Corona to AuNPs via the Poly(dA) Internal Loops. Gold nanospheres are known to noncovalently bind to the poly(dA) via Au-N interactions. ^{19,22,46} To evaluate this binding, we first prepared a AuNP-bound hairpin-based DNA construct. For that, we incubated the DNA construct with 5 nm gold nanospheres at -80 °C for 15 min in a 10:1 mol ratio before thawing at room temperature. ²² This

freeze-thaw procedure enabled the binding of AuNP to the (dA)₂₁ regions in the DNA construct (see sections S7 and S8 and Figure S4 in the Supporting Information). The force ramp experiment was performed after the construct was tethered between the two trapped beads in optical tweezers instrument. During mechanical unfolding of the AuNP bound DNA construct, a new rupture feature at a force higher than that to unfold terminal hairpin (14.9 pN, average force from Figure 1C) or internal loops (12.7 pN, average force from Figure 1C) was observed (state "3" in Figure 2A-C, average 37.0 pN). Close inspection on the ΔL histogram (state "3" in Figure 2D) revealed an average unfolding population of 7.0 nm of this feature, which is much smaller than either the terminal hairpin (15.4 nm) or the internal loops (36.5 nm). This observation, plus the fact that a higher force is required for its unfolding, suggests that this feature is associated with the AuNP binding to the DNA construct.

To confirm that the AuNP is bound to the poly(dA) via the internal loops, we performed a control experiment in which both internal loops contain random nucleotide sequences (see Table S1 in the SI for sequences, and Figure S3 in the SI for predicted lowest energy structures of the hairpins). As shown in Figure 3A, the low- ΔL , high-force population (state "3") is significantly reduced (p < 0.05) from 24.2% (state "3" in Figure 2) to 7.5%. In another experiment, we placed $(dA)_{21}$ only in one strand of the internal loop while keeping random sequence in the other loop strand. As shown in Figure 3B, the population of interest (state "3", 8.7% of entire population) was again significantly smaller (p < 0.05) than the two (dA)₂₁ internal loops. When we reduced $(dA)_{21}$ to $(dA)_{10}$ (Figure 3C) in each internal loop, we found the new species reduced to 8.0% of the total population. Finally, when only one internal loop contains (dA)10, whereas the other loop has a random sequence (Figure 3D), the new species further reduced to 7.4% of the entire population. These experiments indicated that $(dA)_{21}$ in both internal loops are most efficient to bind to the 5 nm AuNP. It is conceivable that closer locations of the two

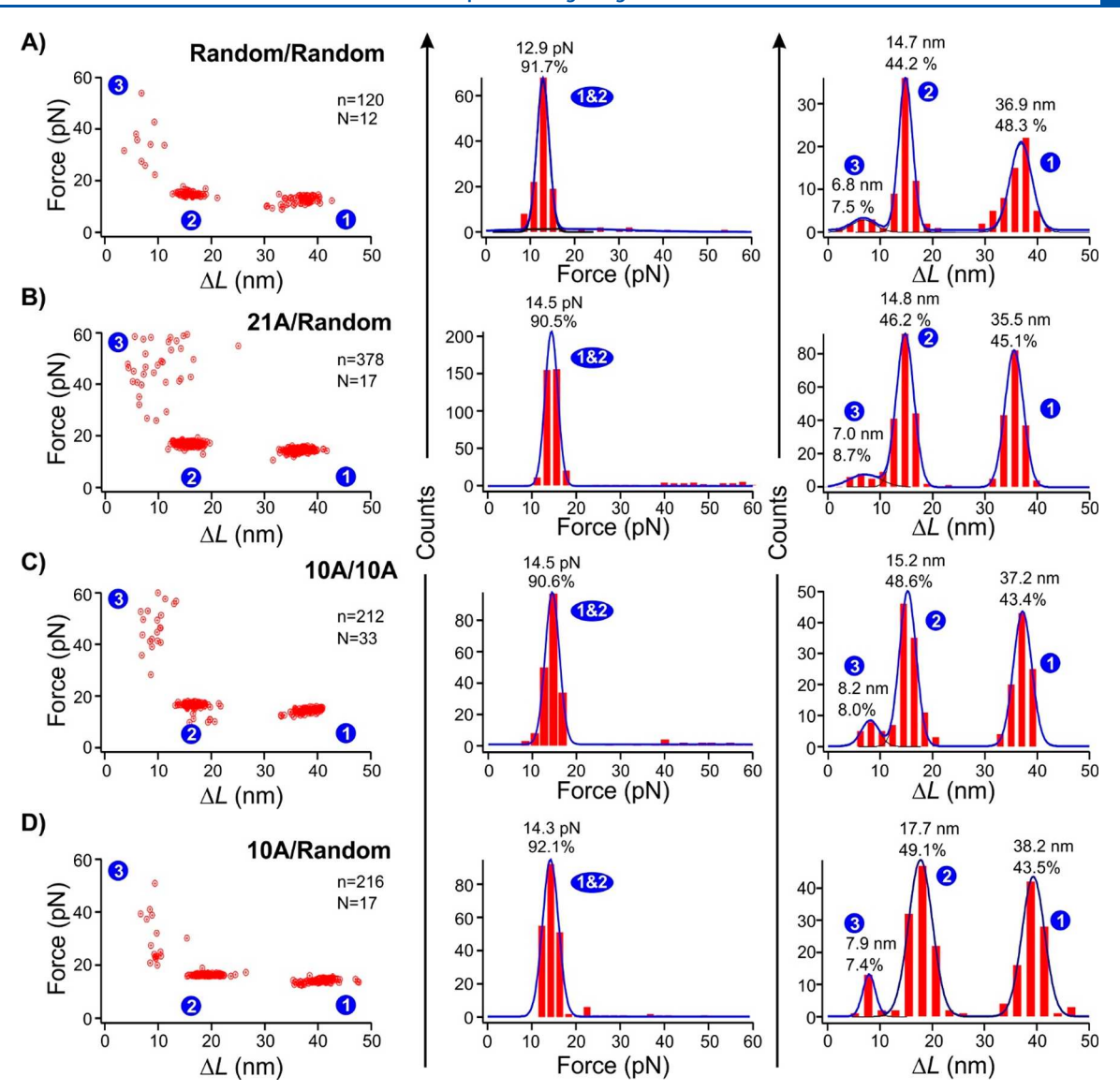


Figure 3. Force vs ΔL plots (left), unfolding force histograms (middle), and ΔL histograms (right) of the unfolding features when the two DNA strands in the internal loops have different poly(dA) sequences: (A) two random sequences, (B) one (dA)₂₁ and one random sequence, (C) two (dA)₁₀ sequences, and (D) one (dA)₁₀ and one random sequence. Solid curves are Gaussian fittings. N represents the number of molecules from which the FX curves were collected, and n represents the total number of unfolding features measured. All experiments were performed in the presence of 5 nm AuNP.

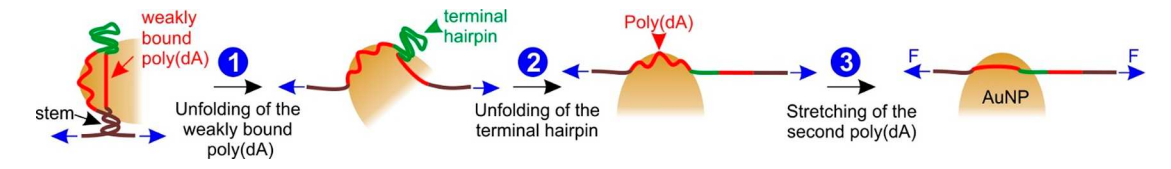


Figure 4. Mechanical desorption pathway of the DNA adsorbed on the AuNP surface. The DNA adsorption is achieved via the two $(dA)_{21}$ internal loops (red). Blue arrows indicate the direction of external forces applied.

poly(dA) strands assist with each other to accommodate their better bindings to the AuNP surface.

The fact that a removal of $(dA)_{21}$ or reduction in the length of the poly(dA) segments results in much reduced AuNP binding population while neither rupture force nor ΔL varies with the length of the poly(dA) suggest that only one AuNP is bound to $(dA)_{21}$ in both internal loops. Atomic force microscopy (AFM) images by others with similar poly(dA) and AuNP interactions also proved the binding of one AuNP

by poly(dA) segment.³² Finally, the observation of only one rupture event with the high-force and low- ΔL feature (state "3" in Figures 2 and 3) in each force—extension curve confirmed the binding of single AuNP for each DNA construct used here.

Binding Model between Gold Nanospheres and Poly(dA). Based on the observations from these control experiments (Figure 3), it is clear that poly(dA) on both strands of the internal loop facilitates the binding of one Au nanosphere. Given that the rupture event corresponding to the

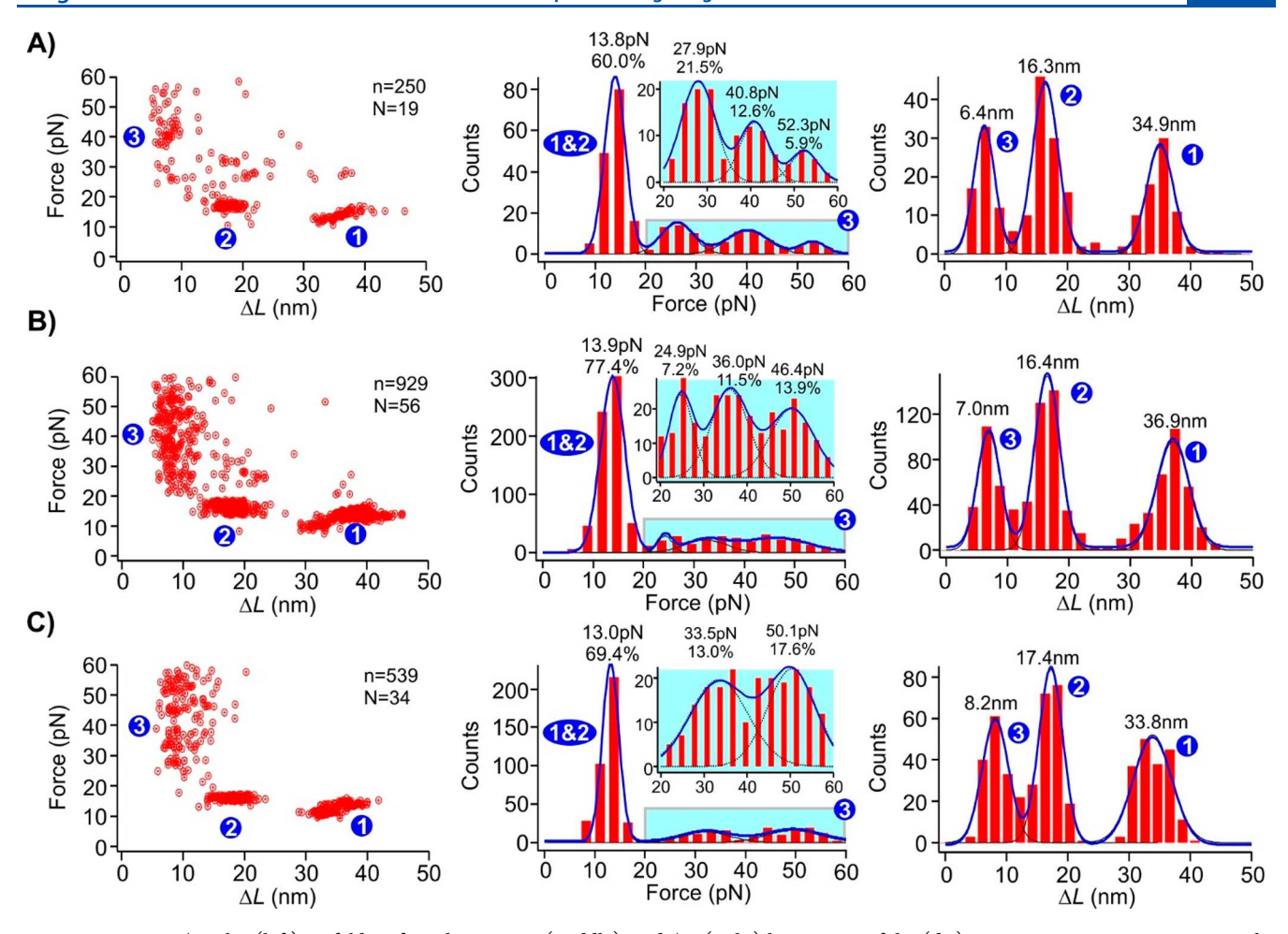


Figure 5. Force vs ΔL plot (left), unfolding force histograms (middle), and ΔL (right) histograms of the (dA)₂₁ containing DNA constructs in the presence of AuNPs with diameters of (A) 1.8, (B) 5.0, and (C) 10.0 nm. Dotted curves in the blown-up insets in the unfolding force histograms represent the Gaussian fits for individual populations. Solid curves are Gaussian fittings for overall populations. N represents the number of molecules from which the FX curves were collected, and n represents the total number of unfolding features measured.

unfolding of the AuNP-DNA conjugate (state "3" in Figure 2) occurs at the later stage of the unfolding sequence where the force is high (Figures 2 and 3), we reasoned that the terminal hairpin (unfolding force = 13.8 pN; see Figure 2C) must unfold before the unbinding of the AuNP-DNA conjugate. This can only occur when one $(dA)_{21}$ strand has a looser binding than the other strand in the internal loops (Figure 4). Thus, the unfolding starts with the ripping of the loosely adsorbed $(dA)_{21}$ strand from the AuNP, generating a large ΔL feature (step 1, Figure 4) with the size and force similar to those without AuNP (compare the state "1" in Figures 1B-D and Figure 2). After step 1, the force experienced by the AuNP-bound DNA construct is exerted on the terminal hairpin (Figure 4). This leads to step 2 in which the unfolding of the terminal hairpin occurs (see state "2" in Figures 2 and 4). Completion of this step results in the force exerted on the remaining $(dA)_{21}$ loop adsorbed to the AuNP. The small ΔL observed during step 3 (7.0 nm, state "3" in Figures 2B and 2D) is either due to the stretching of some looped-out $(dA)_{21}$ region in the DNA-AuNP conjugate or the change in the apparent contour length of the AuNP-bound (dA)₂₁ when the construct experiences higher force (from the winding conformation of the poly(dA) adsorbed to the AuNP surface to the straight conformation; see step 3 in Figure 4).

We argue that, after step 3, the AuNP is still associated with the poly(dA) since steps 1–3 are repeatedly observed in consecutive F-X curves, indicating rebinding of the AuNP to the (dA)₂₁ strands at reduced force. This adsorption is likely due to the Au–N bonds contributed from a limited number of deoxyadenosines without resulting in any looped-out poly(dA) segments. Such an adsorption is not expected to experience significant stretching force in optical tweezers.

Mechanical Binding Strength of the $(dA)_{21}$ to the **AuNPs with Different Sizes.** To study the size effect of the AuNP on the $(dA)_{21}$ binding (state "3" in Figures 1-3 and step 3 in Figure 4), we repeated force-ramping experiments using the hairpin construct with the two (dA)₂₁ internal loops in the presence of Au nanospheres with different sizes. As shown in Figure 5 (state "3"), the unfolding force of the characteristic AuNP-(dA)₂₁ conjugates gradually shifted toward higher force with the increasing nanogold size. With the 1.8 nm nanogold (Figure 5A), the binding populations can be well fit by three force regimes centered at 27.9 pN (21.5%), 40.8 pN (12.6%), and 52.3 pN (5.9%) (average = 36.9 pN). We attribute this distribution to the three possible binding modes between (dA)₂₁ and AuNP (Figure S8 in the Supporting Information). From the unfolding ΔL of 6.4 nm (Figure 5, state "3"), we estimated \sim 16 deoxyadenosines were contained in the sticking-out loop (see Figure S8), leaving five

deoxyadenosines to serve as additional anchoring points (a total of 7) on the AuNP surface. Therefore, the three unfolding force populations in Figure 5A can be attributed to the one, two, or three anchoring deoxyadenosines located on each side of the sticking-out loop, which corresponded the 27.9, 40.8, and 52.3 pN unfolding forces, respectively. Because of the small size of the 1.8 nm AuNP, however, only a limited number of deoxyadenosines can adsorb on AuNP surface. Therefore, the greater the number of anchoring deoxyadenosines, the higher the unfolding force, but the smaller the populations as the random adsorption of all 7 anchoring deoxyadenosines may not be accommodated for the 1.8-nm AuNP. It is likely that, in the most stable binding mode (52.3 pN), the sticking-out poly(dA) loop straddles between two AuNP facets to fully accommodate the 3 anchoring deoxyadenosines on each side (Figure S8).

With the 5.0 nm AuNP (Figure 5B), the three unfolding species (24.9, 36.0, and 46.4 pN, average = 39.5 pN), which respectively correspond to the 1, 2, and 3 anchoring deoxyadenosines on each side of the sticking-out loop (a total of 6 anchoring deoxyadenosines, see Figure S8), increase their populations (7.2%, 11.5%, and 13.9%, respectively). We attribute this to the bigger surface area of the 5-nm nanogold than the 1.8-nm AuNP, which makes it easier for all the anchoring deoxyadenosines to bind to the same AuNP facet (Figure S8), thereby increasing the mechanical stabilities of the adsorbed DNA as well as respective populations. Finally, the DNA adsorbed on the 10.0-nm AuNP showed only two populations (33.5 pN (13.0%) and 50.1 pN (17.6%), average = 42.6 pN; see Figure 5C). This is expected as a maximum of four anchoring deoxyadenosines is allowed in this case (see Figure S8 for calculation). This trend can be explained as larger facets in the 10-nm nanogold have increased the opportunity to accommodate one (the 33.5-pN population) or two (the 50.1-pN species) anchoring deoxyadenosines at each side of the sticking-out loop on the same facet (Figure S8). Since the 33.5-pN population contains only one deoxyadenosine anchored at one side of the sticking-out loop, its force is lower than those of the 1.8-nm (40.8 pN) and 5.0-nm AuNP (36.0 pN), both of which have at least two anchoring deoxyadenosines at each side of the sticking-out loop.

We found that average mechanical stability of $(dA)_{21}$ strands adsorbed on these three AuNPs is ~40 pN. This value is significantly higher than the stall force of DNA/RNA polymerases.^{37–39} Therefore, similar to the G-quadruplex that may serve as a mechanical block^{47,48} to DNA replication or RNA transcription processes, the AuNP-poly(dA) may also serve similar functions, given that there are plenty of poly(dA) segments in genomes of many species.^{41–43} This potential function further expands the applicability of AuNP in biomedicines. This approach of determining the mechanical stability of DNA corona phase on nanoparticles can also be extended to other materials such as carbon nanotubes which are of growing interest in recent years.⁴⁹ However, the use of optical tweezers also comes with the limitation that it cannot measure very high forces, unlike AFM.³⁴

CONCLUSIONS

In summary, we have found the mechanical stability of the DNA corona phase on gold nanospheres increased with the size of AuNP. The average desorption force of the DNA corona is 36.9–42.6 pN, which is lower than the covalent S—Au attachment, but higher than those to maintain DNA duplex

or tetraplex structures inside cells, suggesting that the poly(dA) adsorption on AuNPs can withstand intracellular environment from mechanical perspective. The fact that the desorption force of poly(dA) from AuNP is higher than the stall force of motor proteins brings the possibility of using AuNP as a new agent to modulate various processes catalyzed by motor proteins, which include replication and transcriptions. Given numerous applications of AuNPs inside cells as well as in materials explorations, our findings here provide convincing support that noncovalent DNA corona adsorption can serve as a mechanically competent approach to tailor functions of gold or other nanospheres.

ASSOCIATED CONTENT

Supporting Information

The Supporting Information is available free of charge at https://pubs.acs.org/doi/10.1021/acs.langmuir.2c02251.

Materials; list of oligos; preparation of dsDNA handles for the synthesis of single-molecule hairpin construct; synthesis of single-molecule hairpin construct to study mechanical stability of poly(dA) and AuNPs; $(dA)_{21}$ hairpin structure; predicted structures of the DNA construct studied; binding of gold nanospheres to the poly(dA) containing hairpin-internal-loop construct; UV/vis spectra of AuNP and poly(dA) mixture before and after freeze—thaw process; three-channel microfluidic chamber; mechanochemical study of poly(dA) and AuNP binding in optical tweezers; calculation of the theoretical change-in-contour length (ΔL) of the construct during mechanical unfolding; possible binding modes of the $(dA)_{21}$ to the AuNPs with different sizes (PDF)

AUTHOR INFORMATION

Corresponding Author

Hanbin Mao – Department of Chemistry and Biochemistry and Advanced Materials and Liquid Crystal Institute, Kent State University, Kent, Ohio 44242, United States; orcid.org/0000-0002-6720-9429; Email: hmao@kent.edu

Authors

Pravin Pokhrel – Department of Chemistry and Biochemistry, Kent State University, Kent, Ohio 44242, United States; o orcid.org/0000-0003-4259-6087

Kehao Ren — Department of Chemistry and Biochemistry, Kent State University, Kent, Ohio 44242, United States Hao Shen — Department of Chemistry and Biochemistry, Kent State University, Kent, Ohio 44242, United States; orcid.org/0000-0002-2798-5861

Complete contact information is available at: https://pubs.acs.org/10.1021/acs.langmuir.2c02251

Author Contributions

P.P. and K.R. performed single-molecule experiments. P.P. and H.M. wrote the manuscript. H.M. gave conceptual framework of the experiment. H.S. provided critical feedback and comments on the manuscript. All authors reviewed and gave approval to the final version of the manuscript.

Notes

The authors declare no competing financial interest.

ACKNOWLEDGMENTS

H.M. thanks the National Science Foundation (NSF) (No. CBET1904921) and National Institutes of Health (NIH) (No. R01 CA236350) for the grant support.

REFERENCES

- (1) Giljohann, D. A.; Seferos, D. S.; Daniel, W. L.; Massich, M. D.; Patel, P. C.; Mirkin, C. A. Gold nanoparticles for biology and medicine. *Angew. Chem. (Int. Ed. Engl.)* **2010**, 49, 3280.
- (2) Yeh, Y.-C.; Creran, B.; Rotello, V. M. Gold nanoparticles: preparation, properties, and applications in bionanotechnology. *Nanoscale* **2012**, *4*, 1871.
- (3) Dreaden, E. C.; Alkilany, A. M.; Huang, X.; Murphy, C. J.; El-Sayed, M. A. The golden age: gold nanoparticles for biomedicine. *Chem. Soc. Rev.* **2012**, *41*, 2740.
- (4) Tiwari, P. M.; Vig, K.; Dennis, V. A.; Singh, S. R. Functionalized Gold Nanoparticles and Their Biomedical Applications. *Nanomaterials (Basel, Switz.)* **2011**, *1*, 31.
- (5) Guo, Y.; Wang, Z.; Qu, W.; Shao, H.; Jiang, X. Colorimetric detection of mercury, lead and copper ions simultaneously using protein-functionalized gold nanoparticles. *Biosens. Bioelectron.* **2011**, 26, 4064
- (6) Abad, J. M.; Mertens, S. F. L.; Pita, M.; Fernández, V. M.; Schiffrin, D. J. Functionalization of Thioctic Acid-Capped Gold Nanoparticles for Specific Immobilization of Histidine-Tagged Proteins. J. Am. Chem. Soc. 2005, 127, 5689.
- (7) Zhang, X.; Servos, M. R.; Liu, J. Instantaneous and Quantitative Functionalization of Gold Nanoparticles with Thiolated DNA Using a pH-Assisted and Surfactant-Free Route. *J. Am. Chem. Soc.* **2012**, *134*, 7266.
- (8) Delong, R.; Reynolds, C.; Malcolm, Y.; Schaeffer, A.; Severs, T.; Wanekaya, A. Functionalized gold nanoparticles for the binding, stabilization, and delivery of therapeutic DNA, RNA, and other biological macromolecules. *Nanotechnol., Sci. Appl.* **2010**, *3*, 53–63.
- (9) Mirkin, C. A.; Letsinger, R. L.; Mucic, R. C.; Storhoff, J. J. A DNA-based method for rationally assembling nanoparticles into macroscopic materials. *Nature* **1996**, 382, 607.
- (10) Thomas, K. G.; Kamat, P. V. Chromophore-Functionalized Gold Nanoparticles. *Acc. Chem. Res.* **2003**, *36*, 888.
- (11) Gibson, J. D.; Khanal, B. P.; Zubarev, E. R. Paclitaxel-Functionalized Gold Nanoparticles. *J. Am. Chem. Soc.* **2007**, *129*, 11653.
- (12) Liu, B.; Liu, J. Methods for preparing DNA-functionalized gold nanoparticles, a key reagent of bioanalytical chemistry. *Anal. Methods* **2017**, *9*, 2633.
- (13) Hurst, S. J.; Lytton-Jean, A. K. R.; Mirkin, C. A. Maximizing DNA loading on a range of gold nanoparticle sizes. *Anal. Chem.* **2006**, 78, 8313.
- (14) Storhoff, J. J.; Elghanian, R.; Mucic, R. C.; Mirkin, C. A.; Letsinger, R. L. One-Pot Colorimetric Differentiation of Polynucleotides with Single Base Imperfections Using Gold Nanoparticle Probes. *J. Am. Chem. Soc.* **1998**, *120*, 1959.
- (15) Elghanian, R.; Storhoff, J. J.; Mucic, R. C.; Letsinger, R. L.; Mirkin, C. A. Selective Colorimetric Detection of Polynucleotides Based on the Distance-Dependent Optical Properties of Gold Nanoparticles. *Science* 1997, 277, 1078–1081.
- (16) Li, H.; Rothberg, L. Colorimetric detection of DNA sequences based on electrostatic interactions with unmodified gold nanoparticles. *Proc. Natl. Acad. Sci. U. S. A.* **2004**, *101*, 14036.
- (17) Pei, H.; Li, F.; Wan, Y.; Wei, M.; Liu, H.; Su, Y.; Chen, N.; Huang, Q.; Fan, C. Designed Diblock Oligonucleotide for the Synthesis of Spatially Isolated and Highly Hybridizable Functionalization of DNA-Gold Nanoparticle Nanoconjugates. *J. Am. Chem. Soc.* **2012**, *134*, 11876.
- (18) Opdahl, A.; Petrovykh, D. Y.; Kimura-Suda, H.; Tarlov, M. J.; Whitman, L. J. Independent control of grafting density and conformation of single-stranded DNA brushes. *Proc. Natl. Acad. Sci. U. S. A.* **2007**, *104*, 9.

- (19) Zhu, D.; Song, P.; Shen, J.; Su, S.; Chao, J.; Aldalbahi, A.; Zhou, Z.; Song, S.; Fan, C.; Zuo, X.; Tian, Y.; Wang, L.; Pei, H. PolyA-Mediated DNA Assembly on Gold Nanoparticles for Thermodynamically Favorable and Rapid Hybridization Analysis. *Anal. Chem.* **2016**, 88, 4949.
- (20) Koo, K. M.; Sina, A. A. I.; Carrascosa, L. G.; Shiddiky, M. J. A.; Trau, M. DNA-bare gold affinity interactions: mechanism and applications in biosensing. *Anal. Methods* **2015**, *7*, 7042.
- (21) Zhang, X.; Liu, B.; Dave, N.; Servos, M. R.; Liu, J. Instantaneous Attachment of an Ultrahigh Density of Nonthiolated DNA to Gold Nanoparticles and Its Applications. *Langmuir* **2012**, 28, 17053.
- (22) Hu, M.; Yuan, C.; Tian, T.; Wang, X.; Sun, J.; Xiong, E.; Zhou, X. Single-Step, Salt-Aging-Free, and Thiol-Free Freezing Construction of AuNP-Based Bioprobes for Advancing CRISPR-Based Diagnostics. *J. Am. Chem. Soc.* **2020**, *142*, 7506.
- (23) Li, F.; Zhang, H.; Dever, B.; Li, X.-F.; Le, X. C. Thermal Stability of DNA Functionalized Gold Nanoparticles. *Bioconjugate Chem.* **2013**, 24, 1790.
- (24) Zhou, J.; Ralston, J.; Sedev, R.; Beattie, D. A. Functionalized gold nanoparticles: Synthesis, structure and colloid stability. *J. Colloid Interface Sci.* **2009**, 331, 251.
- (25) Kang, H.; Buchman, J. T.; Rodriguez, R. S.; Ring, H. L.; He, J.; Bantz, K. C.; Haynes, C. L. Stabilization of Silver and Gold Nanoparticles: Preservation and Improvement of Plasmonic Functionalities. *Chem. Rev.* **2019**, *119*, 664.
- (26) Gao, J.; Huang, X.; Liu, H.; Zan, F.; Ren, J. Colloidal Stability of Gold Nanoparticles Modified with Thiol Compounds: Bioconjugation and Application in Cancer Cell Imaging. *Langmuir* **2012**, 28, 4464.
- (27) Mei, B. C.; Oh, E.; Susumu, K.; Farrell, D.; Mountziaris, T. J.; Mattoussi, H. Effects of Ligand Coordination Number and Surface Curvature on the Stability of Gold Nanoparticles in Aqueous Solutions. *Langmuir* **2009**, *25*, 10604.
- (28) Grandbois, M.; Beyer, M.; Rief, M.; Clausen-Schaumann, H.; Gaub, H. E. How Strong Is a Covalent Bond? *Science* **1999**, 283, 1727.
- (29) Huang; Chen, F.; Bennett, P. A.; Tao. Tao Single Molecule Junctions Formed via Au-Thiol Contact: Stability and Breakdown Mechanism. J. Am. Chem. Soc. 2007, 129, 13225.
- (30) Xue, Y.; Li, X.; Li, H.; Zhang, W. Quantifying thiol-gold interactions towards the efficient strength control. *Nat. Commun.* **2014**, *5*, 4348.
- (31) Wei, W.; Sun, Y.; Zhu, M.; Liu, X.; Sun, P.; Wang, F.; Gui, Q.; Meng, W.; Cao, Y.; Zhao, J. Structural Insights and the Surprisingly Low Mechanical Stability of the Au-S Bond in the Gold-Specific Protein Golb. *J. Am. Chem. Soc.* **2015**, *137*, 15358.
- (32) Chen, X.; Wang, Y.; Dai, X.; Ding, L.; Chen, J.; Yao, G.; Liu, X.; Luo, S.; Shi, J.; Wang, L.; Nechushtai, R.; Pikarsky, E.; Willner, I.; Fan, C.; Li, J. Single-Stranded DNA-Encoded Gold Nanoparticle Clusters as Programmable Enzyme Equivalents. *J. Am. Chem. Soc.* **2022**, *144*, 6311.
- (33) Wang, S.-T.; Zhang, H.; Xuan, S.; Nykypanchuk, D.; Zhang, Y.; Freychet, G.; Ocko, B. M.; Zuckermann, R. N.; Todorova, N.; Gang, O. Compact Peptoid Molecular Brushes for Nanoparticle Stabilization. *J. Am. Chem. Soc.* **2022**, *144*, 8138.
- (34) Neuman, K. C.; Nagy, A. Single-molecule force spectroscopy: optical tweezers, magnetic tweezers and atomic force microscopy. *Nat. Methods* **2008**, *5*, 491.
- (35) Woodside, M. T.; Behnke-Parks, W. M.; Larizadeh, K.; Travers, K.; Herschlag, D.; Block, S. M. Nanomechanical measurements of the sequence-dependent folding landscapes of single nucleic acid hairpins. *Proc. Natl. Acad. Sci. U. S. A.* **2006**, *103*, 6190.
- (36) Koirala, D.; Dhakal, S.; Ashbridge, B.; Sannohe, Y.; Rodriguez, R.; Sugiyama, H.; Balasubramanian, S.; Mao, H. A single-molecule platform for investigation of interactions between G-quadruplexes and small-molecule ligands. *Nat. Chem.* **2011**, *3*, 782.
- (37) Galburt, E. A.; Grill, S. W.; Wiedmann, A.; Lubkowska, L.; Choy, J.; Nogales, E.; Kashlev, M.; Bustamante, C. Backtracking

- determines the force sensitivity of RNAP II in a factor-dependent manner. *Nature* **2007**, *446*, 820.
- (38) Wang, M. D.; Schnitzer, M. J.; Yin, H.; Landick, R.; Gelles, J.; Block, S. M. Force and Velocity Measured for Single Molecules of RNA Polymerase. *Science* **1998**, 282, 902.
- (39) Maier, B.; Bensimon, D.; Croquette, V. Replication by a single DNA polymerase of a stretched single-stranded DNA. *Proc. Natl. Acad. Sci. U. S. A.* **2000**, 97, 12002.
- (40) Huppert, J. L.; Balasubramanian, S. Prevalence of quadruplexes in the human genome. *Nucleic Acids Res.* **2005**, *33*, 2908.
- (41) Lustig, A. J.; Petes, T. D. Long poly(A) tracts in the human genome are associated with the Alu family of repeated elements. *J. Mol. Biol.* 1984, 180, 753.
- (42) Shenkin, A.; Burdon, R. H. Deoxyadenylate-rich and deoxyguanylate-rich regions in mammalian DNA. J. Mol. Biol. 1974, 85, 19.
- (43) Tubbs, A.; Sridharan, S.; van Wietmarschen, N.; Maman, Y.; Callen, E.; Stanlie, A.; Wu, W.; Wu, X.; Day, A.; Wong, N.; Yin, M.; Canela, A.; Fu, H.; Redon, C.; Pruitt, S. C.; Jaszczyszyn, Y.; Aladjem, M. I.; Aplan, P. D.; Hyrien, O.; Nussenzweig, A. Dual Roles of Poly(dA:dT) Tracts in Replication Initiation and Fork Collapse. *Cell* **2018**, *174*, 1127.
- (44) Mandal, S.; Zhang, X.; Pandey, S.; Mao, H. Single-Molecule Topochemical Analyses for Large-Scale Multiplexing Tasks. *Anal. Chem.* **2019**, *91*, 13485.
- (45) von Hippel, P. H.; Johnson, N. P.; Marcus, A. H. Fifty years of DNA "Breathing": Reflections on old and new approaches. *Biopolymers* **2013**, *99*, 923.
- (46) Yin, J.; Wang, J.; Yang, X.; Wu, T.; Wang, H.; Zhou, X. Poly(adenine)-mediated DNA-functionalized gold nanoparticles for sensitive detection of mercury ions in aqueous media. *RSC Adv.* **2019**, *9*, 18728.
- (47) Yu, Z.; Schonhoft, J. D.; Dhakal, S.; Bajracharya, R.; Hegde, R.; Basu, S.; Mao, H. ILPR G-Quadruplexes Formed in Seconds Demonstrate High Mechanical Stabilities. *J. Am. Chem. Soc.* **2009**, 131, 1876.
- (48) Mandal, S.; Kawamoto, Y.; Yue, Z.; Hashiya, K.; Cui, Y.; Bando, T.; Pandey, S.; Hoque, M. E.; Hossain, M. A.; Sugiyama, H.; Mao, H. Submolecular dissection reveals strong and specific binding of polyamide-pyridostatin conjugates to human telomere interface. *Nucleic Acids Res.* **2019**, *47*, 3295.
- (49) Cheung, W.; Pontoriero, F.; Taratula, O.; Chen, A. M.; He, H. DNA and carbon nanotubes as medicine. *Adv. Drug Delivery Rev.* **2010**, *62*, *633*.

☐ Recommended by ACS

Stability of End-to-End Base Stacking Interactions in Highly Concentrated DNA Solutions

Sineth G. Kodikara, Hamza Balci, et al.

MARCH 23, 2023

LANGMUIR

READ 🗹

Non-Invasive, Reliable, and Fast Quantification of DNA Loading on Gold Nanoparticles by a One-Step Optical Measurement

Jaewon Lee and Seungwoo Lee

JANUARY 12, 2023

ANALYTICAL CHEMISTRY

READ "

Spherical DNA for Probing Wettability of Microplastics

Mohamad Zandieh, Juewen Liu, et al.

MARCH 29, 2023

LANGMUIR

READ 🗹

Amalgamation of DNAzymes and Nanozymes in a Coronazyme

Li Zuo, Hao Shen, et al.

FEBRUARY 16, 2023

JOURNAL OF THE AMERICAN CHEMICAL SOCIETY

READ 🗹

Get More Suggestions >